



Use of a global model to understand
to understand
speciated
atmospheric mercury
observations

P. Weiss-Penzias et al.

Use of a global model to understand speciated atmospheric mercury observations at five high-elevation sites

P. Weiss-Penzias¹, H. M. Amos², N. E. Selin³, M. Sexauer Gustin⁴, D. A. Jaffe⁵,
D. Obrist⁶, G.-R. Sheu⁷, and A. Giang³

¹Microbiology and Environmental Toxicology, Santa Cruz, California, USA

²School of Public Health, Cambridge, Massachusetts, USA

³Engineering Systems and Atmospheric Chemistry, Cambridge, Massachusetts, USA

⁴Department of Natural Resources and Environmental Science, University of Nevada, Reno, USA

⁵School of Science, Technology, Engineering & Mathematics, USA

⁶Division of Atmospheric Sciences, Reno, Nevada, USA

⁷Department of Atmospheric Sciences, National Central University, Jhongli 320, Taiwan

Received: 17 June 2014 – Accepted: 12 August 2014 – Published: 8 September 2014

Correspondence to: P. Weiss-Penzias (pweiss@ucsc.edu)

Published by Copernicus Publications on behalf of the European Geosciences Union.

Title Page

Abstract

Introduction

Conclusions

References

Tables

Figures



Back

Close

Full Screen / Esc

Printer-friendly Version

Interactive Discussion



Abstract

Atmospheric mercury (Hg) measurements using the Tekran[®] analytical system from 5 high-elevation sites (1400–3200 m elevation), one in Asia and 4 in the western US, were compiled over multiple seasons and years, and these data were compared with the global model GEOS-Chem. Mercury data consisted of gaseous elemental Hg (GEM) and “reactive Hg” (RM) which is a combination of the gaseous oxidized (GOM) and particulate bound (< 2.5 μm) (PBM) fractions as measured by the Tekran[®] system. We used a subset of the observations by defining a “free tropospheric” (FT) dataset by screening using measured water vapor mixing ratios. The oxidation scheme used by the GEOS-Chem model was varied between the standard run with Br oxidation and an alternative run with OH-O₃ oxidation. We used this model-measurement comparison to help interpret the spatio-temporal trends in, and relationships among the Hg species and ancillary parameters and to better understand the sources and fate of atmospheric RM. The most salient feature of the data across sites, seen more in the summer relative to the spring, was that RM was negatively correlated with GEM and water vapor mixing ratios (WV) and positively correlated with ozone (O₃) both in the standard model and for most of the observations, indicating that RM was formed in dry upper altitude air from the photo-oxidation of GEM. Overall, however, the comparison between observed mercury species (GEM and RM) and those from the standard model showed a relatively weak relationship demonstrating the need to strengthen our understanding of fundamental chemistry and measurement artifacts. An improved correlation between the observations and the model was seen when the model was run with the OH-O₃ oxidation scheme instead of the Br oxidation scheme. This simulation produced higher concentrations of RM and lower concentrations of GEM, especially at the desert sites in northwestern Nevada, which raises the possibility that OH as an oxidant via the HgBr+OH pathway could be more important in the summer at desert sites, compared to the mountaintop sites at Storm Peak and Mount Bachelor.

22764

ACPD

14, 22763–22792, 2014

Use of a global model to understand speciated atmospheric mercury observations

P. Weiss-Penzias et al.

Title Page

Abstract

Introduction

Conclusions

References

Tables

Figures

◀

▶

◀

▶

Back

Close

Full Screen / Esc

Printer-friendly Version

Interactive Discussion



1 Introduction

Mercury (Hg) is a neurotoxin that persists in the environment and bioaccumulates in food chains. It is dispersed globally by long-range atmospheric transport (Schroeder and Munthe, 1998; Strode et al., 2008). Anthropogenic sources emit Hg to the atmosphere as gaseous elemental mercury (GEM) and divalent chemical compounds (Hg^{II}), whereas natural sources are thought to emit predominantly GEM (Pirrone et al., 2010). Oxidized atmospheric compounds (also termed Reactive Mercury = RM = Gaseous Oxidized Mercury (GOM) + Particulate Bound Mercury (PBM)) are typically measured as two operationally-defined forms. The first is adsorbed onto a KCl (potassium chloride)-coated denuder and the later collected on a quartz fiber filter and quartz chips (Landis et al., 2002). Gaseous oxidized Hg is water soluble and removed rapidly from the atmosphere in wet deposition (Lindberg and Straton, 1998), however it may be transported long distances in the free troposphere (Huang et al., 2012; Ambrose et al., 2012, Wright et al., 2013). Dry deposition is also thought to be an important sink for GOM and this has been demonstrated using surrogate surfaces. (cf. Gustin et al, 2012; Wright et al, 2013; Huang et al., 2013, Sather et al., 2013, Castro et al., 2013). The lifetime of PBM, limited by particle size, is typically less than 10 days (Schroeder and Munthe, 1998). Gaseous elemental Hg has lower water solubility and an atmospheric lifetime on the order of months to a year (Schroeder and Munthe, 1998). This form may also make a contribution to dry deposition of equivalent magnitude to GOM (Zhang et al., 2012). Gaseous elemental Hg atoms may be re-emitted depending on the surfaces on which they land (Gustin, 2011).

Most measurements of Hg forms made using the Tekran[®] system have found that GEM comprises 95–100 % of total Hg (Valente et al., 2007), a result of the long lifetime of GEM, and the rapid removal of GOM and PBM by wet and dry deposition. However, observations in the free troposphere (FT) from a mountain-top site have shown that the concentrations of GOM can be roughly equivalent to the concentrations of GEM during brief periods (Swartzendruber et al., 2006; Timonen et al., 2013). Observations

2.2 Speciated Hg and ancillary measurements

At all sites GEM, GOM, and PBM were measured with the Tekran[®] 2537/1130/1135 automated CVAFS instrument. Details of the Hg measurements, along with O₃ and meteorology are described in detail elsewhere (Swartzendruber et al., 2006; Faïn et al., 2009; Peterson et al., 2009; Lyman and Gustin, 2008; Sheu et al., 2010). Briefly, air is drawn into an inlet with a 2.5 μm size cut impactor into a KCl-coated denuder which absorbs GOM (unknown efficiency), then through a quartz fiber filter and quartz chips which are hypothesized to collect PBM, and finally across alternating Au cartridges which adsorb GEM. Gaseous elemental Hg measurements are recorded every 5 min, while GOM and PBM are collected for 2 h and desorbed for 1 h, giving a measurement every 3 h.

GEM can be calibrated with a primary source, but currently there is no calibrant for GOM or PBM, a serious limitation to the accuracy of all data produced by the Tekran[®] system (Gustin and Jaffe, 2010; Jaffe et al., 2014). Furthermore, ambient ozone concentrations negatively interfere with the adsorption and retention of GOM on the denuder (Lyman et al., 2010). There is also recent evidence that GOM may be composed of various forms of Hg, including HgCl₂, HgBr₂, etc., and that the KCl-coated denuder may not collect all these forms with equivalent efficiency (Gustin et al., 2012, 2013; Huang et al., 2013). In addition to the denuder, some fraction of GOM may be collected on the quartz fiber filter in the particulate Hg instrument (Tekran[®]-1135) (Gustin et al., 2013), and for these reasons we present GOM + PBM=reactive Hg (RM) measurements in this paper. A recent inter-comparison between Tekran[®] and new Hg measurement methods was performed and it was found that the Tekran[®] RM measurements were systematically 2–3 times lower than Hg^{II} measured with other methods (Gustin et al., 2013; Huang et al., 2013). Thus, the Tekran[®] measurements reported in this paper, while representing the best available observations, must be treated with caution in light of these uncertainties, and are likely a lower bound to the actual concentrations of RM. However, despite these uncertainties, speciated Hg data from these

Use of a global model to understand speciated atmospheric mercury observations

P. Weiss-Penzias et al.

Title Page

Abstract

Introduction

Conclusions

References

Tables

Figures

◀

▶

◀

▶

Back

Close

Full Screen / Esc

Printer-friendly Version

Interactive Discussion



high-elevation sites might still be meaningful for comparing site-to-site variability and RM/GEM slopes.

2.3 GEOS-Chem model

The standard model runs used version 9-01-01 of the GEOS-Chem (GC) Hg coupled atmosphere-ocean-land model (www.geos-chem.org), described in detail elsewhere (Amos et al., 2012). Briefly, the simulation was conducted for 2004–2009 with GEOS-5 assimilated meteorological and surface data from the NASA Global Modeling and Assimilation Office (GMAO) at the $2^\circ \times 2.5^\circ$ resolution. The GEOS-Chem simulation transports 2 Hg tracers in the atmosphere: Hg and Hg^{II}. Mercury redox chemistry followed Holmes et al. (2010), with oxidation of Hg by Br atoms and photoreduction of Hg^{II} in liquid cloud droplets. Oxidation of Hg by OH and O₃ is an alternative to oxidation by Br in GEOS-Chem (Holmes et al., 2010). The likelihood that OH-O₃ oxidation would proceed in the atmosphere has been questioned (Hynes et al., 2009; Goodsite et al., 2004). However, given the large uncertainties surrounding the oxidation of GEM, we include model runs with OH-O₃ oxidation mechanism as a model test to shed light on potential shortcomings of the Br mechanism. Anthropogenic emissions are from GEIA 2005 inventory (Pacyna et al., 2010). Model output is taken from pressure levels consistent with each site, and mean modeled values, on seasonal, daily, 12 h, and 3 h timescales, were compared with observations. Ancillary model output data (O₃, WV, and T) were generated from the v9-01-01 full chemistry simulation. GEOS-Chem has been extensively evaluated against Mercury Deposition Network wet deposition observations (Amos et al., 2012; Holmes et al., 2010; Selin and Jacob, 2008) as well as surface land-based sites, ship cruises, and plane flight data of GEM and seawater concentrations (Selin et al., 2008; Holmes et al. 2010; Soerensen et al., 2010; Amos et al., 2012).

Use of a global model to understand speciated atmospheric mercury observations

P. Weiss-Penzias et al.

Title Page

Abstract

Introduction

Conclusions

References

Tables

Figures

◀

▶

◀

▶

Back

Close

Full Screen / Esc

Printer-friendly Version

Interactive Discussion



2.4 FT subset of data based on water vapor measurements

The global chemical transport model used here cannot resolve local effects that sometimes influenced the measurements at each site. The model is sampling in the free troposphere (FT) but each site has time periods where the air is from the boundary layer (BL) influenced by surface Hg sources and sinks. In order to compare the Hg observed and modeled data more directly, the observations were filtered using a WV cutoff: only data were considered (termed “FT”) when WV < 75th percentile based on seasonal data sets (Table S1 in the Supplement). The seasonal months were: March–May = spring, June–August = summer, September–November = fall, and December–February = winter. This cutoff removed from the data set, for example, time periods when GEM concentration were > 6 ng m⁻³ at one site in Nevada (NV02). By removing the outliers, the interspecies correlation statistics were more comparable with the model. Applying a more stringent WV cutoff, such as < 50th percentile, would select data with even less influence from the BL, but would have less statistical power due to small numbers of observations. Thus, the 75th percentile WV cutoff was chosen for all sites. Water vapor screens have been used previously based on the empirically-derived equations described in Bolton (1980):

$$WV \left(\text{g kg}^{-1} \right) = \left[\text{RH} \cdot (6.22) \frac{0.01 \cdot e^{\left(77.345 + 0.00577 T_{\text{amb}} - \frac{7235}{T_{\text{amb}}} \right)}}{T_{\text{amb}}^{8.2}} \right] \left(P^{-1} \right)$$

where RH is relative humidity, T_{amb} is the ambient temperature in Kelvin, and P is the barometric pressure in hPa (Weiss-Penzias et al., 2006, 2009; Ambrose et al., 2011; Faïn et al., 2009; Sheu et al., 2010). Since barometric pressure data were not available for each site, a constant P was assumed for each site, based on the elevation of each site, which adds < 1 % error to the WV calculation.

2.5 Statistical analyses

Statistical calculations were performed with Origin 9.1. Comparisons between population means were considered significantly different based on a paired t test or ANOVA with $p < 0.05$. Correlations between species in the observations and the model used daily means to avoid biases associated with diel variations. The model output and the observations were compared over equivalent time periods on the same time resolution.

3 Results and discussion

3.1 Spatial and temporal trends in the observations

Mean measured GEM concentration was highest at LABS during the spring (2.2 ng m^{-3}) likely due to Asian outflow impacting the island of Taiwan during this season (Sheu et al., 2010) (Fig. 1). The lowest observed seasonal mean GEM concentration occurred at DRI during the summer at 1.36 ng m^{-3} , simultaneous with the highest observed RM measurements suggesting photochemical conversion of GEM (Weiss-Penzias et al., 2009). Summertime GEM was lower compared to all other seasons at the sites with measurements in multiple seasons (MBO, DRI, LABS, SPL). The mean GEM concentrations from the unfiltered data set were larger than from the FT data set at NV02 (summer) and DRI (summer), but the opposite trend was observed at MBO (spring) and LABS (spring). This suggests the desert sites were influenced more by local surface sources (Lyman and Gustin, 2008) whereas MBO and LABS have observed springtime Asian long-range transport of GEM in the FT (Jaffe et al., 2005; Sheu et al., 2010).

Measured RM concentrations varied by a about a factor of 7 between sites, with the highest concentrations occurring during summertime dry air conditions at DRI, MBO and SPL (Fig. 1). At the tropical site (LABS), summertime RM was at its seasonal minimum due to high humidity and rapid loss from wet deposition, but during the spring RM

**Use of a global model
to understand
speciated
atmospheric mercury
observations**

P. Weiss-Penzias et al.

[Title Page](#)[Abstract](#)[Introduction](#)[Conclusions](#)[References](#)[Tables](#)[Figures](#)[◀](#)[▶](#)[◀](#)[▶](#)[Back](#)[Close](#)[Full Screen / Esc](#)[Printer-friendly Version](#)[Interactive Discussion](#)

the summer, and the standard model reproduced this RM/GEM trend at all sites (except for LABS) (Figs. 2, 3, Table S2 in the Supplement). Positive slopes were observed between observed RM and O_3 at all sites (significant at MBO, NV02, and SPL) during the summer, and this trend was duplicated by the standard model (significant at all sites). Negative slopes between RM and WV were also observed (significant at all sites except SPL) and modeled (significant at all sites) for data from the summer. Negative correlations of RM with GEM and WV and positive correlations of RM with O_3 both in the observations and the standard are consistent with RM being formed in the free troposphere (where WV was low and O_3 was high) from the photo-oxidation of GEM (resulting in low GEM).

In contrast to the summer time period, however, there was a greater lack of agreement between the model and observations for the spring data in Fig. 2 and Table S2 in the Supplement. The slopes of interspecies correlations of observed RM with GEM were about a factor of 2 less negative during the spring compared to the summer at MBO and SPL (Fig. 2). At LABS, the spring RM/GEM ratio was a factor of 4 less negative compared to the summertime ratio, and at DRI the RM/GEM ratio was positive (Fig. 2). Modeled RM/GEM ratios did not show the same seasonal trend, but instead were similar across spring and summer (~ -275 for MBO, ~ -150 for DRI and $\sim -350 \text{ pg ng}^{-1}$ for SPL). For RM : O_3 the observed ratios were positive and the observed RM : WV ratios were negative at all sites during the summer, but during the spring, these ratios did not show a consistent pattern (e.g. the observed positive correlation between RM and WV during the spring at MBO) (Fig. 2). One or more of the following conditions could account for the seasonal change in the model-observation comparison: (1) a seasonal change in transport of RM from regions other than the free troposphere that was not simulated in the model, (2) unknown oxidation mechanisms that are not included in the model (Timonen et al., 2013), and (3) a seasonal change in chemical forms of RM that were more poorly detected by the analytical system.

3.3 Case study of free tropospheric transport

This study also compared observed and modeled data on 12 h time resolution during a period of subsiding air across western North America (see weather maps and back trajectories shown in Supplement) when observed RM concentrations were elevated. This event occurred during the week of 20–25 June 2007, when 12 h maximum concentrations of the RM reached 26, 250, and 100 pg m^{-3} at MBO, DRI, and NV02, respectively (Fig. 4a, f, i). These maximum values were observed at the 3 sites sequentially in time along a west–east transect from central Oregon to northern Nevada. Maximum RM concentrations occurred at MBO during the night when downslope flow was observed, and maximum RM concentrations at DR and NV02 occurred during the day when convective mixing was at its maximum.

Observed 12 h mean GEM concentrations associated with the RM maxima were 1.0, 1.2, and 1.0 ng m^{-3} at MBO, DRI, and NV02, respectively (Fig. 4b, e, h), all significantly lower than the seasonal means of GEM at each site. The diurnal pattern in GEM can be seen in Fig. 4e and 4h for DRI and NV02, with higher concentrations during the night (12:00 UTC) and lower concentrations during the day (0:00 UTC) due to accumulation in the boundary layer and local geologic emission of GEM.

Observed O_3 concentrations were elevated (> 50 ppb) at DRI and NV02 (Fig. 4d, g) during the RM peak of the event, but at MBO the O_3 concentration was far below seasonal mean (23 ppb) (Fig. 4a), as previously noted by Timonen et al. (2013). However, the O_3 concentrations at MBO rebounded to nearly 50 ppb just after the RM peak, coinciding with the minimum in WV on 22 June 2007 and perhaps lack of mixing with marine boundary layer air.

Observed water vapor concentrations at DRI and NV02 (Fig. 4d, g) were equivalent to, or lower than WV observed at MBO (Fig. 4a), corresponding to minimum relative humidity values of 17%, 6%, and 3%, at MBO, DRI, and NV02 respectively. This indicates the very dry conditions in the desert and may have contributed to the longer

Use of a global model to understand speciated atmospheric mercury observations

P. Weiss-Penzias et al.

Title Page

Abstract

Introduction

Conclusions

References

Tables

Figures

◀

▶

◀

▶

Back

Close

Full Screen / Esc

Printer-friendly Version

Interactive Discussion

oxidation mechanism in the atmosphere. Thus, we ran GEOS-Chem with the OH-O₃ kinetics to see where the Br mechanism might be deficient. Daily mean RM and GEM concentrations from the observations at MBO and DRI and the two model runs are shown in Fig. 5. Note that the standard and OH-O₃ models provide similar RM concentrations but different GEM concentrations. RM concentrations are controlled by deposition and GEM oxidation, and because of the different patterns of oxidants between the OH/O₃ chemistry and Br chemistry, there are different patterns of wet deposition. Reactive Hg concentrations are similar in the two models perhaps due to a compensating effect from wet deposition, whereas GEM is not wet deposited, so its concentrations are reflecting chemistry only and are relatively different between model types.

The correlations across the time series in Fig. 5 between observations and each model run for RM and GEM for the two sites, are shown in Fig. 6. For GEM, the OH-O₃ model more closely matched the observations (steeper slope) compared to the Br model, especially for the data from DRI (Fig. 6). For RM the OH-O₃ model also produced steeper slopes and larger R^2 values compared to the Br model, most notably at DRI. Simulated RM concentrations from the Br model were notably smaller than the observed ones during the summer at DRI. This is significant because RM is probably already a lower bound on real ambient concentrations due to inefficiencies associated with the collection method.

Figure 7 shows monthly mean RM/GEM ratios in the observations plotted against monthly mean RM/GEM ratios in the model using the Br-oxidation scheme (left panel) and the OH-O₃ oxidation scheme (right panel). Excluding LABS, both the observations and the model agree that the higher RM/GEM ratios occurred in the summer months, and lower RM/GEM ratios occurred in the spring and fall. This is consistent with greater photochemical conversion of GEM and greater loss via dry deposition during the spring (Sigler et al., 2009). Modeled RM/GEM using either oxidation scheme was on average 2.8 ± 2.6 higher than the mean observed RM/GEM, a factor roughly in line with the estimate of collection inefficiency of the KCl-denuder (Gustin et al., 2013). Interestingly, however, the RM/GEM ratios using the Br-oxidation scheme fall into two patterns: data

Use of a global model to understand speciated atmospheric mercury observations

P. Weiss-Penzias et al.

Title Page

Abstract

Introduction

Conclusions

References

Tables

Figures

◀

▶

◀

▶

Back

Close

Full Screen / Esc

Printer-friendly Version

Interactive Discussion



collection efficiency of the method. The variability of seasonal mean observed RM concentrations across sites was about a factor of 7 with the highest concentrations seen at DRI and at MBO in the summer and the lowest at LABS in the summer. The standard model also simulated mean RM concentrations that varied by about a factor of 7 across sites, but these concentrations were offset positively from the observations by a mean factor of 2.5 across all sites. However, the model offset was not equivalent at all sites, with mean observed RM concentrations across 3 consecutive summers at DRI being slightly higher than RM concentrations from the standard model (76 vs. 72 pg m^{-3}). This is in contrast to the mean summer RM concentrations at MBO from the observation and the model being 64 and 135 pg m^{-3} , respectively. When the model was run with the OH-O₃ oxidation scheme instead of the Br oxidation scheme, it was found that mean concentrations of RM were higher and GEM were lower, especially at the desert sites DRI and NV02, producing better correlations between measured/modeled RM and GEM compared to the model with the Br-oxidation scheme. This indicates that OH as an oxidant via the HgBr+OH pathway could be more important in the summer at desert sites, compared to the mountaintop sites at MBO and SPL, and suggests that there is not one single global oxidant for GEM and hence multiple forms of RM in the atmosphere.

The Supplement related to this article is available online at doi:10.5194/acpd-14-22763-2014-supplement.

Acknowledgements. The authors wish to thank SPL personnel Gannet Hallar, Ian McCubbin, and Xavier Faïn, and the Taiwan Environmental Protection Administration for financially supporting the atmospheric Hg monitoring at LABS. We would also like to thank the past UNR graduate students that collected the DRI and NV02 data, Seth Lyman and Christiana Peterson. N. E. Selin acknowledges NSF Atmospheric Chemistry Program award 1053648.

Use of a global model to understand speciated atmospheric mercury observations

P. Weiss-Penzias et al.

Title Page

Abstract

Introduction

Conclusions

References

Tables

Figures

◀

▶

◀

▶

Back

Close

Full Screen / Esc

Printer-friendly Version

Interactive Discussion



References

- Ambrose, J. L., Reidmiller, D. R., and Jaffe, D. A.: Causes of high O₃ in the lower free troposphere over the Pacific Northwest as observed at the Mt. Bachelor Observatory, *Atmos. Environ.*, 45, 5302–5315, 2011.
- 5 Ambrose, J. L., Lyman, S. N., Huang, J. Gustin, M. S., and Jaffe, D. A.: Fast time resolution oxidized mercury measurements during the Reno Atmospheric Mercury Intercomparison Experiment (RAMIX), *Environ. Sci. Technol.*, 47, 7285–7294, 2013.
- Amos, H. M., Jacob, D. J., Holmes, C. D., Fisher, J. A., Wang, Q., Yantosca, R. M., Corbitt, E. S., Galarneau, E., Rutter, A. P., Gustin, M. S., Steffen, A., Schauer, J. J., Graydon, J. A., Louis, V. L. St., Talbot, R. W., Edgerton, E. S., Zhang, Y., and Sunderland, E. M.: Gas-particle partitioning of atmospheric Hg(II) and its effect on global mercury deposition, *Atmos. Chem. Phys.*, 12, 591–603, doi:10.5194/acp-12-591-2012, 2012.
- 10 Bolton, D.: The computation of equivalent potential temperature, *Mon. Weather Rev.*, 108, 1046–1053, 1980.
- 15 Castro, M. S., Moore, C., Sherwell, J., and Brooks, S. B.: Dry deposition of gaseous oxidized mercury in Western Maryland, *Sci. Total. Environ.*, 417, 23–40, 2012.
- Dibble, T. S., Zelic, M. J., and Mao, H.: Corrigendum to “Thermodynamics of reactions of ClHg and BrHg radicals with atmospherically abundant free radicals” published in *Atmos. Chem. Phys.* 12, 10271–10279, 2012, *Atmos. Chem. Phys.*, 13, 9211–9212, doi:10.5194/acp-13-9211-2013, 2013.
- 20 Faïn, X., Obrist, D., Hallar, A. G., Mccubbin, I., and Rahn, T.: High levels of reactive gaseous mercury observed at a high elevation research laboratory in the Rocky Mountains, *Atmos. Chem. Phys.*, 9, 8049–8060, doi:10.5194/acp-9-8049-2009, 2009.
- Goodsite, M., Plane, J., and Skov, H.: A theoretical study of the oxidation of Hg⁰ to HgBr₂ in the troposphere, *Environ. Sci. Technol.*, 38, 1772–1776, doi:10.1021/es034680s, 2004.
- 25 Gustin, M. S.: Exchange of mercury between the atmosphere and terrestrial ecosystems, in: *Environmental Chemistry and Toxicology of Mercury*, edited by: Liu, G, Cai, Y, and O’Driscoll, N., John Wiley and Sons, Hoboken, New Jersey, USA, 42–52, 2011.
- Gustin, M. S. and Jaffe, D. A.: Reducing the uncertainty in measurement and understanding of mercury in the atmosphere, *Environ. Sci. Technol.*, 44, 2222–2227, 2010.
- 30 Gustin, M. S., Huang, J., Miller, M. B., Finley, B. D., Call, K., Ambrose, J. L., Peterson, C., Lyman, S. N., Everhart, S., Bauer, D., Remeika, J., Hynes, A., Jaffe, D. A., and Lindberg, S. E.:

Use of a global model to understand speciated atmospheric mercury observations

P. Weiss-Penzias et al.

Title Page

Abstract

Introduction

Conclusions

References

Tables

Figures

◀

▶

◀

▶

Back

Close

Full Screen / Esc

Printer-friendly Version

Interactive Discussion



**Use of a global model
to understand
speciated
atmospheric mercury
observations**

[P. Weiss-Penzias et al.](#)

[Title Page](#)[Abstract](#)[Introduction](#)[Conclusions](#)[References](#)[Tables](#)[Figures](#)[◀](#)[▶](#)[◀](#)[▶](#)[Back](#)[Close](#)[Full Screen / Esc](#)[Printer-friendly Version](#)[Interactive Discussion](#)

RAMIX – a step towards understanding mercury atmospheric chemistry and Tekran[®] observations, *Environ. Sci. Technol.*, 47, 7295–7306, 2013.

Hall, B.: The gas phase oxidation of elemental mercury by ozone, *Water Air Soil Poll.*, 80, 301–315, 1995.

5 Holmes, C., Jacob, D., and Yang, X.: Global lifetime of elemental mercury against oxidation by atomic bromine in the free troposphere. *Geophys. Res. Lett.*, 33, L20808, doi:10.1029/2006GL027176, 2006.

Holmes, C. D., Jacob, D. J., Corbitt, E. S., Mao, J., Yang, X., Talbot, R., and Slemr, F.: Global atmospheric model for mercury including oxidation by bromine atoms, *Atmos. Chem. Phys.*, 10, 12037–12057, doi:10.5194/acp-10-12037-2010, 2010.

10 Huang, J. Y. and Gustin, M. S.: Evidence for a free troposphere source of mercury in wet deposition in the western United States, *Environ. Sci. Technol.*, 46, 6621–6629, 2012.

Huang, J. Y., Miller, M. B., Weiss-Penzias, P., and Gustin, M. S.: Comparison of reactive mercury measurements made with KCl-coated denuders, nylon membranes, and cation exchange membranes, *Environ. Sci. Technol.*, 47, 7307–7316, 2013.

15 Hynes, A. J., Donohoue, D. L., Goodsite, M. E., and Hedgecock, I. M.: Our current understanding of major chemical and physical processes affecting mercury dynamics in the atmosphere and at the air-water/terrestrial interfaces, in: *Mercury Fate and Transport in the Global Atmosphere*, edited by: Mason, R. and Pirrone, N., Springer, New York, 427–457, 2009.

20 Jaffe, D., Prestbo, E., Swartzendruber, P., Weiss-Penzias, P., Kato, S., Takami, A., Hatakeyama, S., and Kajii, Y.: Export of atmospheric mercury from Asia, *Atmos. Environ.*, 39, 3029–3038, 2005.

Jaffe, D., Lyman, S., Amos, H., Gustin, M., Huang, J., Selin, N., Levin, L., Ter Schure, A., Mason, R., Talbot, R., Rutter, A., Finley, B., Jaeglé, L., Shah, V., McClure, C., Ambrose, J., Gratz, L., Lindberg, S., Weiss-Penzias, P., Sheu, G.-R., Feddersen, D., Horvat, M., Dastoor, A., Hynes, A., Mao, H., Sonke, J., Slemr, F., Fisher, J., Ebinghaus, R., Zhang, Y., and Edwards, G.: Progress on understanding atmospheric mercury hampered by uncertain measurements, *Environ. Sci. Technol.*, 48, 7204–7206, 2014.

25 Kos, G., Ryzhkov, A., Dastoor, A., Narayan, J., Steffen, A., Ariya, P. A., and Zhang, L.: Evaluation of discrepancy between measured and modelled oxidized mercury species, *Atmos. Chem. Phys.*, 13, 4839–4863, doi:10.5194/acp-13-4839-2013, 2013.

**Use of a global model
to understand
speciated
atmospheric mercury
observations**

P. Weiss-Penzias et al.

Title Page

Abstract

Introduction

Conclusions

References

Tables

Figures

◀

▶

◀

▶

Back

Close

Full Screen / Esc

Printer-friendly Version

Interactive Discussion



Landis, M. S., Stevens, R. K., Schaedlich, F., and Prestbo, E. M.: Development and characterization of an annular denuder methodology for the measurement of divalent inorganic reactive gaseous mercury in ambient air, *Environ. Sci. Technol.*, 36, 3000–3009, 2002.

Lindberg, S. E. and Stratton, W. J.: Atmospheric mercury speciation: concentrations and behavior of reactive gaseous mercury in ambient air, *Environ. Sci. Technol.*, 32, 49–57, 1998.

Lyman, S. N. and Gustin, M. S.: Speciation of atmospheric mercury at two sites in northern Nevada, USA, *Atmos. Environ.*, 42, 927–939, doi:10.1016/j.atmosenv.2007.10.012, 2008.

Lyman, S. N. and Jaffe, D. A.: Formation and fate of oxidized mercury in the upper troposphere and lower stratosphere, *Nat. Geosci.*, 5, 114–117, doi:10.1038/NGEO1353, 2011.

Lyman, S. N., Jaffe, D. A., and Gustin, M. S.: Release of mercury halides from KCl denuders in the presence of ozone, *Atmos. Chem. Phys.*, 10, 8197–8204, doi:10.5194/acp-10-8197-2010, 2010.

Moore, C. W., Obrist, D., and Luria, M.: Atmospheric mercury depletion events at the Dead Sea: Spatial and temporal aspects, *Atmos. Environ.*, 69, 231–239, 2013.

Moore, C. W., Obrist, D., Steffen, A., Staebler, R., Douglas, T., Richter, A., and Nghiem, S.: Convective forcing of mercury and ozone in the Arctic boundary layer induced by leads in sea ice, *Nature*, 506, 81–84, doi:10.1038/nature12924, 2014.

Murphy, D. M., Hudson, P. K., Thompson, D. S., Sheridan, P. J., and Wilson, J. C.: Observations of mercury-containing aerosols, *Environ. Sci. Technol.*, 40, 3163–3167, 2006.

Obrist, D., Hallar, A. G., McCubbin, I., Stephens, B. B., and Rahn, T.: Atmospheric mercury concentrations at Storm Peak Laboratory in the Rocky Mountains: evidence for long-range transport from Asia, boundary layer contributions, and plant mercury uptake, *Atmos. Environ.*, 42, 7579–7589, doi:10.1016/j.atmosenv.2008.06.051, 2008.

Pacyna, E. G., Pacyna, J. M., Sundseth, K., Munthe, J., Kindbom, K., Wilson, S., Steenhuisen, F., and Maxson, P.: Global emission of mercury to the atmosphere from anthropogenic sources in 2005 and projections to 2020, *Atmos. Environ.*, 44, 2487–2499, doi:10.1016/j.atmosenv.2009.06.009, 2010.

Peterson, C., Gustin, M., and Lyman, S.: Atmospheric mercury concentrations and speciation measured from 2004 to 2007 in Reno, Nevada, USA, *Atmos. Environ.*, 43, 4646–4654, 2009.

Pirrone, N., Cinnirella, S., Feng, X., Finkelman, R. B., Friedli, H. R., Leaner, J., Mason, R., Mukherjee, A. B., Stracher, G. B., Streets, D. G., and Telmer, K.: Global mercury emissions to the atmosphere from anthropogenic and natural sources, *Atmos. Chem. Phys.*, 10, 5951–5964, doi:10.5194/acp-10-5951-2010, 2010.

Use of a global model to understand speciated atmospheric mercury observations

P. Weiss-Penzias et al.

Title Page

Abstract

Introduction

Conclusions

References

Tables

Figures

◀

▶

◀

▶

Back

Close

Full Screen / Esc

Printer-friendly Version

Interactive Discussion



Sather, M.E., Mukerjee, S., Smith, L., Mathew, J., Jackson, C., Callison, R., Scrapper, L., Hathcoat, A., Adam, J., Keese, D., Ketcher, P., Brunette, R., Calstrom, J., and Van der Jagt, G.: Gaseous oxidized mercury dry deposition measurements in the Four Corners Area and Eastern Oklahoma, USA, *Atmos. Pollut. Res.*, 4, 168–180, 2013.

5 Sexauer Gustin, M., Weiss-Penzias, P. S., and Peterson, C.: Investigating sources of gaseous oxidized mercury in dry deposition at three sites across Florida, USA, *Atmos. Chem. Phys.*, 12, 9201–9219, doi:10.5194/acp-12-9201-2012, 2012.

Schroeder, W. H. and Munthe, J.: Atmospheric mercury – an overview, *Atmos. Environ.*, 32, 809–822, 1998.

10 Selin, N. E. and Jacob, D. J.: Seasonal and spatial patterns of mercury wet deposition in the United States: constraints on the contribution from North American anthropogenic sources, *Atmos. Environ.*, 42, 519–5204, doi:10.1016/j.atmosenv.2008.02.069, 2008.

Selin, N. E., Jacob, D. J., Yantosca, R. M., Strode, S., Jaeglé, L., and Sunderland, E. M.: Global 3-D land-ocean-atmosphere model for mercury: Present-day vs. preindustrial cycles and anthropogenic enrichment factors for deposition, *Global Biogeochem. Cyc.*, 22, 1–13, doi:10.1029/2007GB003040, 2008.

Sheu, G.-R., Lin, N.-H., Wang, J.-L., Lee, C.-T., Ou Yang, C.-F., and Wang, S.-H.: Temporal distribution and potential sources of atmospheric mercury measured at a high-elevation background station in Taiwan. *Atmos. Environ.*, 44, 2393–2400, 2010.

20 Sheu, G.-R., Lin, N.-H., Lee, C.-T., Wang, J.-L., Chuang, M.-T., Wang, S.-H., Chi, K. H., and Ou Yang, C.-F.: Distribution of atmospheric mercury in northern Southeast Asia and South China Sea during Dongsha Experiment, *Atmos. Environ.*, 78, 174–183, doi:10.1016/j.atmosenv.2012.07.002, 2012.

Sigler, J. M., Mao, H., and Talbot, R.: Gaseous elemental and reactive mercury in Southern New Hampshire, *Atmos. Chem. Phys.*, 9, 1929–1942, doi:10.5194/acp-9-1929-2009, 2009.

25 Soerensen, A. L., Skov, H., Jacob, D. J., Soerensen, B. T., and Johnson, M. S.: Global concentrations of gaseous elemental mercury and reactive gaseous mercury in the marine boundary layer, *Environ. Sci. Technol.*, 44, 42–427, 2010.

30 Strode, S. A., Jaeglé, L., Jaffe, D. A., Swartzendruber, P. C., Selin, N. E., Holmes, C., and Yantosca, R. M.: Trans-Pacific transport of mercury, *J. Geophys. Res.*, 113, D15305, doi:10.1029/2007JD009428., 2008.

**Use of a global model
to understand
speciated
atmospheric mercury
observations**

P. Weiss-Penzias et al.

[Title Page](#)[Abstract](#)[Introduction](#)[Conclusions](#)[References](#)[Tables](#)[Figures](#)[◀](#)[▶](#)[◀](#)[▶](#)[Back](#)[Close](#)[Full Screen / Esc](#)[Printer-friendly Version](#)[Interactive Discussion](#)

Subir, M., Ariya, P. A., and Dastoor, A. P.: A review of uncertainties in atmospheric modeling of mercury chemistry I. Uncertainties in existing kinetic parameters: fundamental limitations and the importance of heterogeneous chemistry, *Atmos. Environ.*, 45, 5664–5676, 2011.

Swartzendruber, P. C., Jaffe, D. A., Prestbo, E. M., Weiss-Penzias, P., Selin, N. E., Park, R., Jacob, D. J., Strode, S., and Jaeglé, L.: Observations of reactive gaseous mercury in the free troposphere at the Mount Bachelor Observatory. *J. Geophys. Res.*, 111, D24301, doi:10.1029/2006JD007415, 2006.

Swartzendruber, P. C., Chand, D., Jaffe, D. A., Smith, J., Reidmiller, D., Gratz, L., Keeler, J., Strode, S., Jaeglé, L., and Talbot, R.: Vertical distribution of mercury, CO, ozone, and aerosol scattering in the Pacific Northwest during the spring 2006 INTEX-B campaign, *J. Geophys. Res.*, 113, D10305, doi:10.1029/2007JD009579, 2008.

Talbot, R., Mao, H., Scheuer, E., Dibb, J., and Avery, M.: Total depletion of Hg0 in the upper troposphere-lower stratosphere, *Geophys. Res. Lett.*, 34, L23804, doi:10.1029/2007GL031366, 2007.

Timonen, H., Ambrose, J. L., and Jaffe, D. A.: Oxidation of elemental Hg in anthropogenic and marine airmasses, *Atmos. Chem. Phys.*, 13, 2827–2836, doi:10.5194/acp-13-2827-2013, 2013.

Valente, R. J., Shea, C., Humes, K. L., and Tanner R. L.: Atmospheric mercury in the Great Smoky Mountains compared to regional and global levels. *Atmos. Environ.*, 41, 1861–1873, 2007.

Weiss-Penzias, P., Jaffe, D. A., Swartzendruber, P., Dennison, J. B., Chand, D., Hafner, W., and Prestbo, E.: Observations of Asian air pollution in the free troposphere at Mount Bachelor Observatory during the spring of 2004, *J. Geophys. Res.*, 111, D10304, doi:10.1029/2005JD006522, 2006.

Weiss-Penzias, P., Gustin, M. S., and Lyman, S. N.: Observations of speciated atmospheric mercury at three sites in Nevada: evidence for a free tropospheric source of reactive gaseous mercury, *J. Geophys. Res.*, 114, D14302, doi:10.1029/2008JD011607, 2009.

Wright, G., Miller, M. B., Weiss-Penzias, P., Gustin, M.: Investigation of mercury deposition and potential sources at six sites from the Pacific Coast to the Great Basin, USA, *Sci. Total Environ.*, 470–471C, 1099–1113, doi:10.1016/j.scitotenv.2013.10.071, 2014.

Zhang, L., Blanchard P., Johnson, D., Dastoor, A., Ryzhkov, A., Lin, C. J., Vijayaraghavan, K., Gay, D., Holsen, T. M., Huang, J., Graydon, J. A., St. Louis, V. L., Castro, M. S., Miller, E. K.,

Marsik, F., Lu, J., Poissant, L., Pilote, M., and Zhang, K. M.: Assessment of modeled mercury dry deposition over the Great Lakes region, Environ. Pollut, 161, 272–283, 2012.

ACPD

14, 22763–22792, 2014

Use of a global model to understand speciated atmospheric mercury observations

P. Weiss-Penzias et al.

Title Page

Abstract

Introduction

Conclusions

References

Tables

Figures



Back

Close

Full Screen / Esc

Printer-friendly Version

Interactive Discussion



Use of a global model to understand speciated atmospheric mercury observations

P. Weiss-Penzias et al.

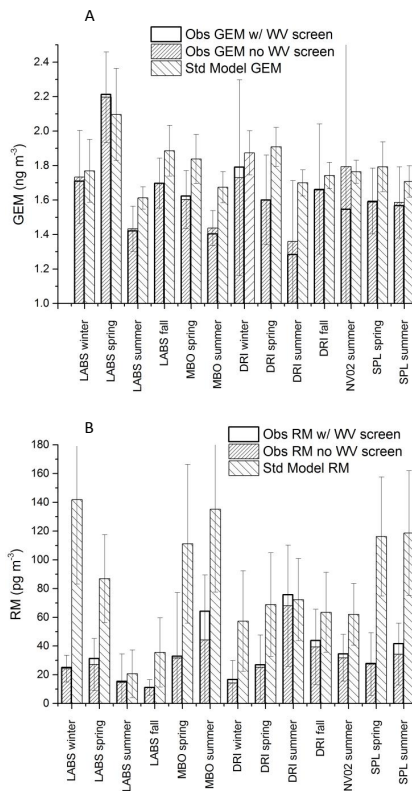


Figure 1. Means and standard deviations of observed and standard-modeled **(A)** GEM and **(B)** RM for each site by season. The WW screened data are plotted in the same column as the unscreened data.

Title Page

Abstract Introduction

Conclusions References

Tables Figures

◀ ▶

◀ ▶

Back Close

Full Screen / Esc

Printer-friendly Version

Interactive Discussion



Use of a global model to understand speciated atmospheric mercury observations

P. Weiss-Penzias et al.

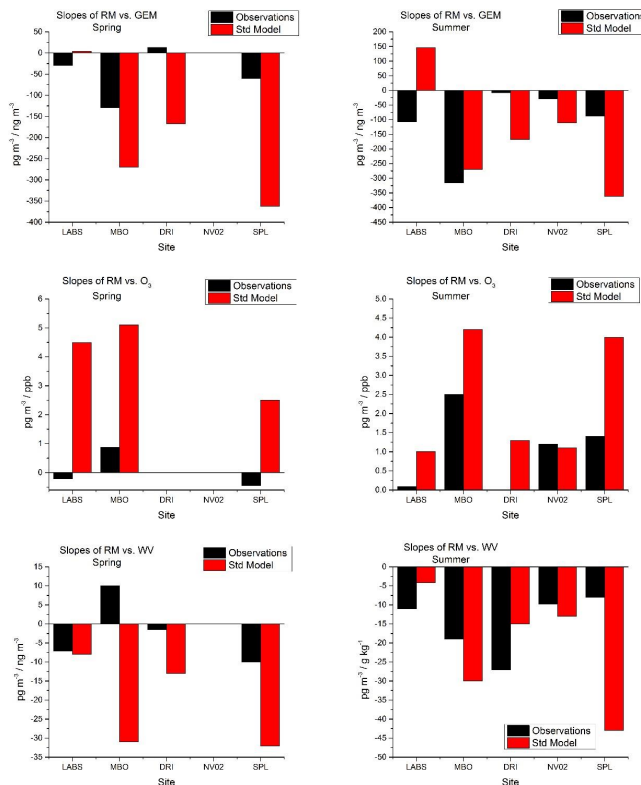


Figure 2. Slopes from the linear regressions of observed and standard-modeled RM vs. GEM, RM vs. O₃, and RM vs. water vapor daily mean concentrations for each site and season. Observed data were filtered using only data when WV < 75th percentile. Winter and fall data not shown. All linear regression statistics given in Table S2 in the Supplement.

Title Page

Abstract Introduction

Conclusions References

Tables Figures

◀ ▶

◀ ▶

Back Close

Full Screen / Esc

Printer-friendly Version

Interactive Discussion



Use of a global model to understand speciated atmospheric mercury observations

P. Weiss-Penzias et al.

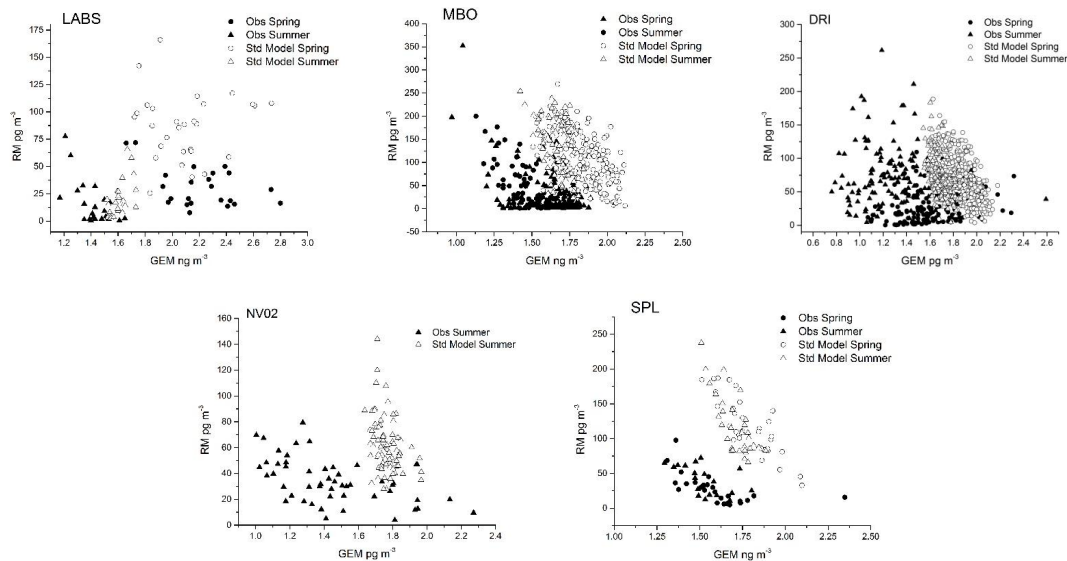


Figure 3. Scatter plots of RM vs. GEM daily mean concentrations for the WV-screened observations and the standard model delineated by site and season.

Title Page

Abstract

Introduction

Conclusions

References

Tables

Figures



Back

Close

Full Screen / Esc

Printer-friendly Version

Interactive Discussion



Use of a global model to understand speciated atmospheric mercury observations

P. Weiss-Penzias et al.

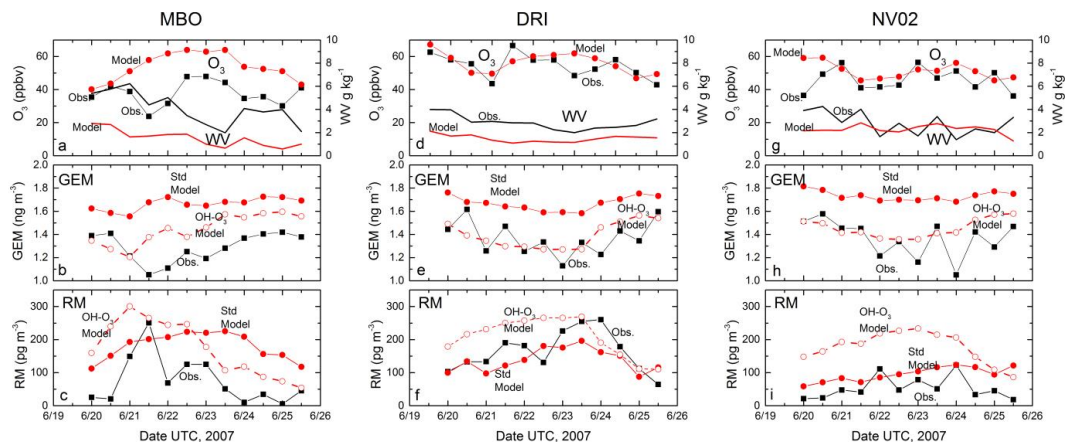


Figure 4. Twelve-hour mean concentrations of O_3 , water vapor, GEM, and RM at three sites during a high-RM event during 20–25 June 2007. Observational, standard model, and OH– O_3 model data are shown.

Title Page

Abstract

Introduction

Conclusions

References

Tables

Figures

◀

▶

◀

▶

Back

Close

Full Screen / Esc

Printer-friendly Version

Interactive Discussion

Use of a global model to understand speciated atmospheric mercury observations

P. Weiss-Penzias et al.

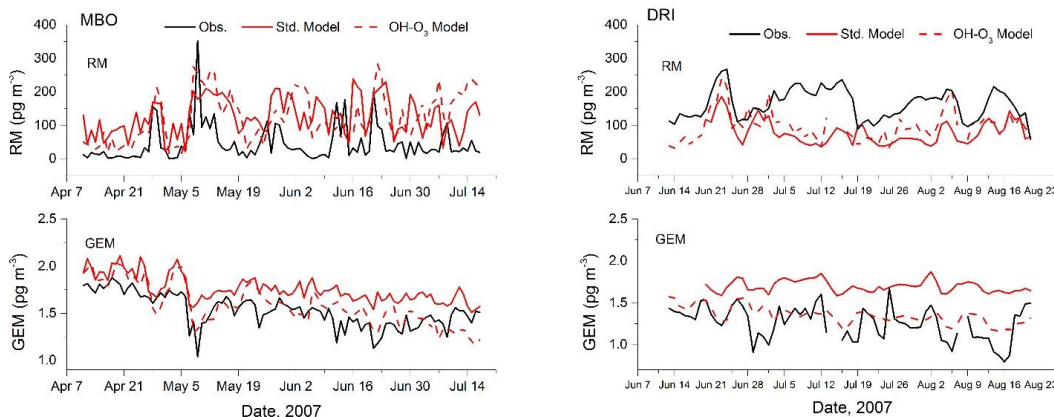


Figure 5. Comparison of observed, standard-modeled, and OH–O₃-modeled RM and GEM daily mean concentrations for spring/summer 2007 at MBO and summer 2007 at DRI.

Title Page

Abstract

Introduction

Conclusions

References

Tables

Figures

◀

▶

◀

▶

Back

Close

Full Screen / Esc

Printer-friendly Version

Interactive Discussion



Use of a global model to understand speciated atmospheric mercury observations

P. Weiss-Penzias et al.

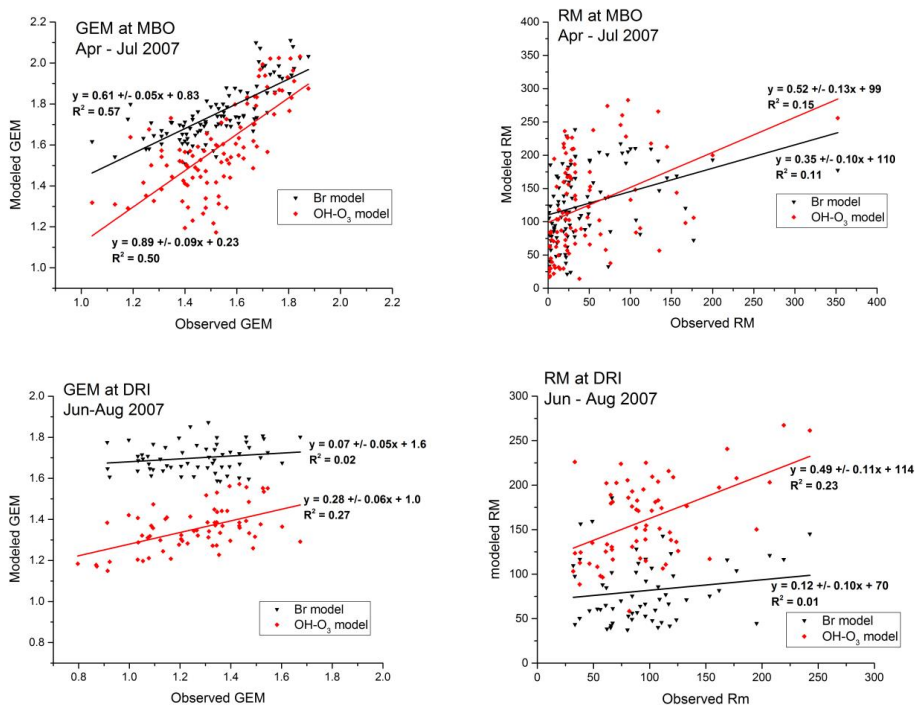


Figure 6. Comparison of linear relationships between GEM and RM in the observations with data from the model using either the Br or the OH–O₃ oxidation schemes.

Title Page

Abstract Introduction

Conclusions References

Tables Figures

◀ ▶

◀ ▶

Back Close

Full Screen / Esc

Printer-friendly Version

Interactive Discussion



